TMAO Promotes Fibrillization and Microtubule Assembly Activity in the C-Terminal Repeat Region of Tau[†]

Francesca Scaramozzino,[‡] Dylan W. Peterson,[‡] Patrick Farmer,[‡] J. T. Gerig,[§] Donald J. Graves,[‡] and John Lew*[,‡]

Department of Molecular, Cellular, and Developmental Biology, University of California, Santa Barbara, California 93106, and Department of Chemistry and Biochemistry, University of California, Santa Barbara, California 93106

Received October 23, 2005; Revised Manuscript Received December 15, 2005

ABSTRACT: Alzheimer's disease most closely correlates with the appearance of the neurofibrillary tangles (NFTs), intracellular fibrous aggregates of the microtubule-associated protein, tau. Under native conditions, tau is an unstructured protein, and its physical characterization has revealed no clues about the three-dimensional structural determinants essential for aggregation or microtubule binding. We have found that the natural osmolyte trimethylamine *N*-oxide (TMAO) induces secondary structure in a C-terminal fragment of tau (tau^{187}) and greatly promotes both self-aggregation and microtubule (MT) assembly activity. These processes could be distinguished, however, by a single-amino acid substitution (Tyr^{310} → Ala), which severely inhibited aggregation but had no effect on MT assembly activity. The inability of this mutant to aggregate could be completely reversed by TMAO. We propose a model in which TMAO induces partial order in tau^{187}, resulting in conformers that may correspond to on-pathway intermediates of either aggregation or tau-dependent MT assembly or both. These studies set the stage for future high-resolution structural characterization of these intermediates and the basis by which Tyr^{310} may direct pathologic versus normal tau function.

Alzheimer's disease (AD)[1] is characterized by the appearance of two biochemical lesions: the extracellular amyloid plaques and the intracellular neurofibrillary tangles. However, it is the accumulation of the latter due to aggregation of the microtubule-associated protein, tau, that correlates most closely with disease progression (*1*). The normal function of tau is the stabilization and organization of microtubules (MTs), but under pathological conditions, tau undergoes protein misfolding, leading to self-aggregation and fiber formation (*1*, *2*). The molecular mechanisms that govern the folding of tau to its normal state, as opposed to the pathological formation of fibers, are unknown.

Tau, under native conditions, exists as an unfolded, highly flexible "random coil" (*3*−*7*). This is evidenced by a negative maximum around 200 nm in the CD spectrum, a peak at ∼1645 cm^{-1} (amide I band) in the FTIR spectrum, the absence of a clearly defined radius of gyration by X-ray scattering, and an unusually large Stokes radius determined by hydrodynamic methods (*3*−*5*, *7*, *8*) and by NMR studies of selected tau peptides (*9*−*12*). As a consequence of its unstructured nature, tau has resisted all attempts to crystallize it for X-ray diffraction studies. Recently, multidimensional NMR analysis of the MT-binding domain of tau has revealed significant β-structure in regions that are critical for aggregation (*13*).

Paired helical filaments (PHFs) can be assembled in vitro from soluble, recombinant tau, typically in the presence of either polyanionic cofactors such as heparin or surfactants such as arachidonic acid (*14*). In contrast to monomeric tau, tau fibrils display significant secondary structure. Most studies report predominant β-sheet or cross-β-sheet structure in fibers generated from recombinant tau or PHF-tau isolated from brain (*15*−*19*), while two studies to date report significant α-helical content (*20*, *21*). Nonetheless, the presence of secondary structural elements in fibers suggests that significant folding occurs during aggregation.

The folding pathway through which tau assembles into filaments has been described on only a macroscopic level (*22*). The mechanism of aggregation in vitro can be described in three steps. The first step in the reaction is the stabilization of an assembly competent intermediate that can be detected by enhanaced thioflavin T (ThT) fluorescence (*22*, *23*). On the basis of its reactivity with ThT, it has been proposed that this intermediate represents a partially folded form of tau containing enriched β-sheet structure. The intermediate appears before filament nucleation and is prone to self-association. In the second step of aggregation, the assembly reaction proceeds through an exponential growth phase. Finally, net growth ceases, resulting in a constant polymer mass in which filaments undergo steady-state assembly and/or disassembly.

The native structure of a protein is influenced critically by its solvent environment (*24*). Certain organisms that have adapted to extreme environments have evolved small organic

[†] This work was supported by a grant from the National Institutes of Health (GM0580445).

* To whom correspondence should be addressed: Department of Molecular, Cellular, and Developmental Biology, University of California, Santa Barbara, CA 93106. Telephone: (805) 893-5336. Fax: (805) 893-4724. E-mail: lew@lifesci.ucsb.edu.

[‡] Department of Molecular, Cellular, and Developmental Biology.

[§] Department of Chemistry and Biochemistry.

[1] Abbreviations: AD, Alzheimer's disease; MT, microtubule; TMAO, trimethylamine *N*-oxide; CD, circular dichroism; PHF, paired helical filaments; ThT, thioflavin T.

10.1021/bi052167g CCC: $33.50
Published on Web 03/01/2006

metabolites (osmolytes) that stabilize and protect intracellular proteins from denaturation due to harsh environmental stresses (*25*). A remarkable feature of these osmolytes is that they retain their ability to promote the folding of naturally unstructured or denatured proteins into their native structures and, thus, act as chemical chaperones in the absence of denaturing environmental stresses. The chemical basis for protein stabilization by such osmolytes is best attributed to an osmophobic effect that arises from the unfavorable interaction of the protein backbone with osmolyte (*26*). While specific protection of the native state is believed to be an evolved function, the stabilizing effect of osmolytes is generic to all proteins even if they did not evolve in the presence of the osmolyte (*25*, *27*, *28*). Trimethylamine *N*-oxide (TMAO) is an osmolyte found in marine elasmobranchs (sharks and rays) (*29*) as well as in mammalian kidney cells (*30*), which has evolved for protection against the denaturing effects of high levels of endogenous urea. In vitro, the chaperone activity of TMAO has been demonstrated in a number of systems (*31*−*34*), including reduced carboxyamidated RNase T1 and a destabilized mutant of staphylococcal nuclease A, systems in which unfolded ensembles dominate under native conditions but which attain nativelike structure and function in the presence of TMAO (*35*). The cumulative data suggest that TMAO may serve as a useful tool in the study of structure and function in proteins that are naturally unstructured under physiological conditions.

Herein, we report that TMAO induces conformational reorganization in a C-terminal fragment of tau and dramatically accelerates both aggregation/fiber formation and tau-dependent microtubule assembly. A point substitution, $Y^{310}A$, profoundly inhibits aggregation but has no effect on tau-dependent microtubule assembly. The defect in aggregation caused by this mutation can be completely reversed by TMAO. Characterization of the critical conformer induced by TMAO using high-resolution methods may be a crucial step in our understanding of the structural basis for tau aggregation.

EXPERIMENTAL PROCEDURES

Chemicals and Tau^{187} Protein. Full-length tau and a C-terminal fragment of human tau corresponding to residues 255−441 (tau^{187}) were overexpressed in *Escherichia coli* using the pET vector expression system (Novagen). The mutant [Y^{310}A]tau^{187} was prepared using the standard protocol of the Quickchange mutagenesis kit (Stratagene). Proteins were purified by heat treatment followed by P11 phosphocellulose chromatography followed by reverse phase HPLC, as previously described (*36*). The homogeneity of tau proteins was analyzed by SDS−PAGE. Full-length tau and tau^{187} concentrations were determined from the sum of extinction coefficients of individual tyrosine residues at 280 nm. Heparin (average MW of 18 000) and thioflavin T were from Sigma. Trimethylamine oxide dehydrate was obtained from Sigma.

Fluorescence Measurements of Aggregation. Purified tau was centrifuged at 52000*g* for 30 min. Polymerization was initiated by addition of 0.11 mg/mL heparin to a 200 μL solution containing protein at different concentrations, 20 mM potassium phosphate buffer (pH 7), 1 mM DTT, and 25 μM ThT. Changes in ThT fluorescence were monitored using an excitation wavelength of 450 nm and an emission wavelength of 480 nm with a Fluorolog-3 spectrofluorometer (Jobin Yvon-Spex), using a 3 mm semimicro quartz cell. Measurements were carried out at 25 °C.

Transmission Electron Microscopy. Negative stain EM was performed in a JEOL 1230 instrument operated at 80 kV. Ten microliters of aggregation mix [0.11 mg/mL heparin, 20 mM potassium phosphate buffer (pH 7), and 1 mM DTT], which contained 10 μM tau^{187} incubated with or without TMAO, was applied to a carbon-coated copper grid for 90 s, and then the grid was rinsed with H_2O. Cytochrome *c* was applied for 20 s, and the grid was rinsed and then stained with 1.5% uranyl acetate for 20 s.

Tubulin Assembly. Tubulin purified from bovine brain by a standard procedure (Mitchison, 1984) was kindly provided by L. Wilson. Tubulin assembly (at 25 °C) was monitored using absorbance at 350 nm as a measure of turbidity in a Shimadzu (UV-1601) spectrophotometer as described by Tseng (*37*). In brief, tubulin was thawed and then centrifuged at 15000*g* for 10 min at 4 °C. The supernatant was collected and used for assembly reactions. Assembly was initiated by the addition of tubulin (5 μM) in the presence or absence of 200 mM TMAO, 1.5 μM tau, or 5 μM paclitaxel; 1 mM GTP, 1 mM DTT, 1 mM $MgCl_2$, 1 mM EGTA, 0.1 mM EDTA, and 100 mM Mes (pH 6.4) were always present.

Circular Dichroism Spectroscopy. CD spectra were obtained using an AVIV 202 CD spectrometer. All measurements were carried out at 25 °C in a 1 mm path length cell. The scanning speed was 1 nm/s with a bandwidth of 1.0 nm and a response time of 0.5 s. Background spectra of the solvent mixture were recorded and subtracted from all spectra.

Nuclear Magnetic Resonance. Proton NMR spectra were collected at 500 MHz using a Varian INOVA instrument. NMR samples contained 0.8 mM protein, 10 mM potassium phosphate buffer (pH 6.5), and 10% D_2O. TMAO was used at 1.6 M. The sample temperature was controlled at 25 °C and calibrated using a standard sample of methanol. NOESY spectra were collected using a method similar to that of Fulton and Ni (*38*) except that the water flip-back pulse was omitted. Double solvent signal suppression (water and TMAO) was done with samples containing TMAO (*39*).

RESULTS

TMAO Induces Structure in Tau^{187}. Human tau under native conditions is best described as an unstructured molecule when free in solution (*3*−*7*). Common wisdom predicts that the formation of secondary or tertiary structural elements is a prerequisite for biological function in proteins in general. Given the known effects of TMAO on the folding of proteins, we asked how TMAO may affect the folding of a C-terminal fragment of human tau in terms of promoting organized structure leading to function in this molecule. This fragment (tau^{187}) contains the complete MT-binding repeat region (from residue 255 to the end) and promotes assembly of tubulin into microtubules. In addition, tau^{187} undergoes heparin-induced aggregation to form fibers reminiscent of those found in AD brain tissue.

Analysis by circular dichroism (CD) spectroscopy of tau^{187} confirms an unstructured protein (Figure 1), consistent with existing structural information about full-length tau (*4*, *8*).

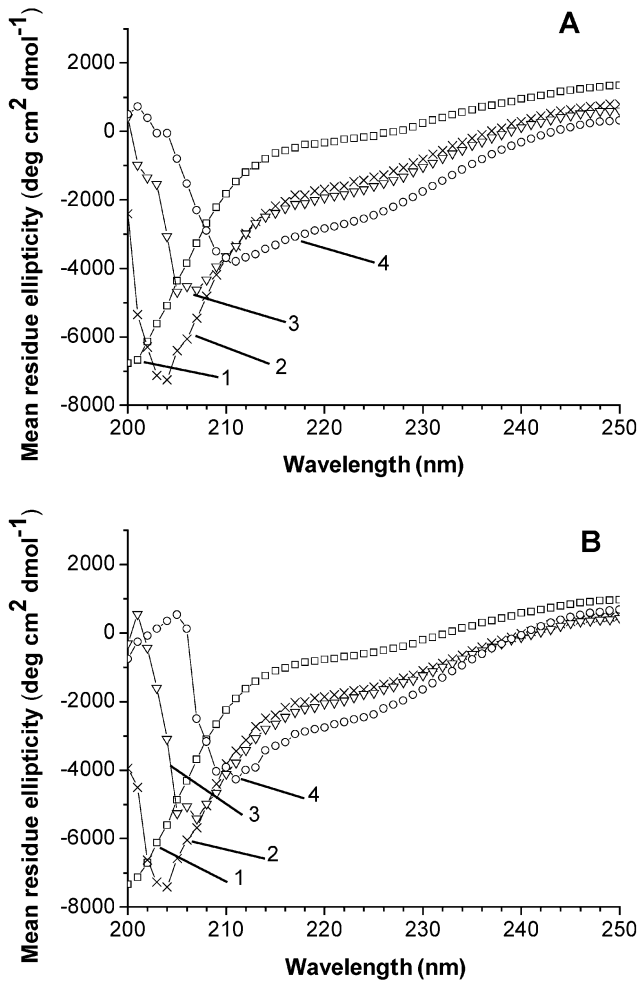

FIGURE 1: Circular dichroism spectroscopy of tau^{187} and [Y^{310}A]-tau^{187} as a function of TMAO concentration. CD spectra of wild-type tau^{187} or [Y^{310}A]tau^{187} (each at 40 μM) were acquired in 10 mM potassium phosphate buffer (pH 6.8) at 25 °C, in the absence of heparin. (A) Wild-type tau^{187} alone (□) (trace 1) and tau^{187} with 0.2 M TMAO (×) (trace 2), 1 M TMAO (▽) (trace 3), or 2 M TMAO (○) (trace 4). (B) [Y^{310}A]Tau^{187} alone (□) (trace 1) and [Y^{310}A]tau^{187} with 0.2 M TMAO (×) (trace 2), 1 M TMAO (▽) (trace 3), or 2 M TMAO (○) (trace 4). The experiment was repeated at least three times.

The unfolded nature of tau^{187} is indicated by a negative peak around 200 nm (*40*). In the presence of TMAO (from 200 mM to 2 M), circular dichroism experiments revealed a significant increase in the level of secondary structure, defined principally by the transition of the molar ellipticity at 200 nm from negative to positive values, and a shift in the spectrum to longer wavelengths (Figure 1). A broad peak at ~215 nm, typical of β-structure, and a small shoulder at 222 nm, typical of β-turns, develop with an increase in TMAO concentration. It was not possible to estimate the relative secondary structure composition of tau in the presence of TMAO, due to the strong interfering absorbance of TMAO at wavelengths of <200 nm.

The increase in the level of structure in tau^{187} suggested by the CD data in response to TMAO is supported by proton NMR analysis. Figure 2 compares the fingerprint regions of tau^{187} in the absence and presence of TMAO. The narrow dispersion of the alpha and peptide chemical shifts in both spectra is consistent with a largely unstructured polypeptide, probably undergoing interchange through a range of conformations. Although site-specific assignments of chemical shifts cannot be made using these data, it is clear that TMAO alters the composition of the mix of conformers present, as reflected by a significant number of altered chemical shifts. There are more CαH−NH cross-peaks apparent for tau^{187} in the presence of TMAO, a situation that may arise because TMAO slows the rates of some conformational interconversions, leading to narrow spectral lines of some conformations since more CαH−NH cross-peaks are apparent in the presence of TMAO. A similar effect of TMAO on spectra of a molten globule state has recently been reported (*41*).

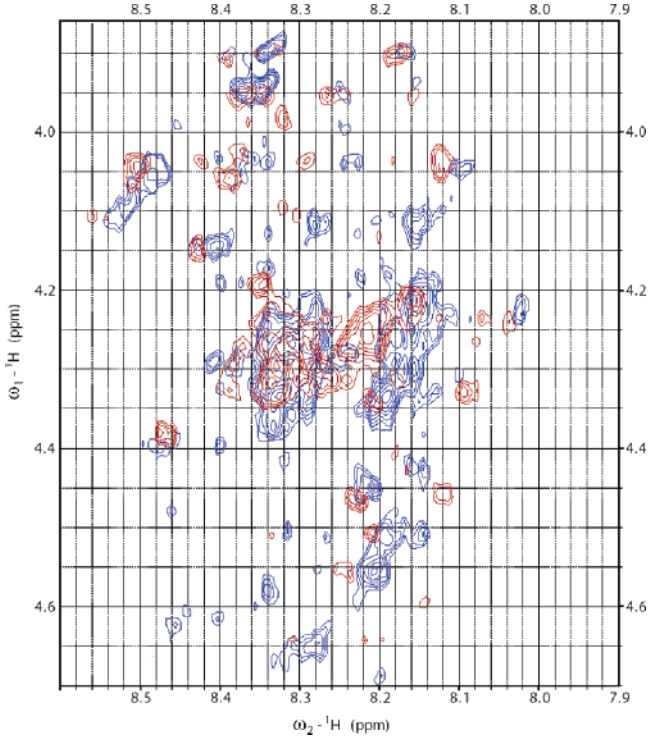

FIGURE 2: Proton NMR spectroscopy at 500 MHz. Fingerprint region of NOESY spectra from the tau^{187} fragment in the absence (red) and presence (blue) of 1.6 M TMAO at 25 °C. The protein concentration was 0.8 mM; the pH was 6.0. The NOESY mixing time was 200 ms. The experiment was repeated more than three times.

TMAO Enhances the Ability of Tau^{187} To Promote Microtubule Assembly. The chaperone activity of TMAO has previously been demonstrated by the enhanced ability that this agent confers on full-length tau to promote MT assembly (*37*, *42*−*44*). Consistent with reports about full-length tau, we observed a robust increase in the rate of MT assembly promoted by tau^{187} in the presence of 200 mM TMAO (Figure 3). However, neither our data nor those previously published discern whether these effects of TMAO are attributable to effects specifically on tau, tubulin, or both. We therefore asked if TMAO could enhance the assembly of MTs induced to polymerize by paclitaxel. Figure 3 shows that TMAO has essentially no effect on the kinetics of MT assembly when polymerization is initiated with paclitaxel instead of tau. Although it is possible that the mechanisms of paclitaxel- versus tau-induced MT assembly may be distinct, these data suggest that TMAO acts specifically on tau to enhance its MT assembly activity.

TMAO Promotes Aggregation of Tau^{187}. We investigated the effects of TMAO on the kinetics of tau^{187} aggregation. The time course of aggregation was followed by thioflavin

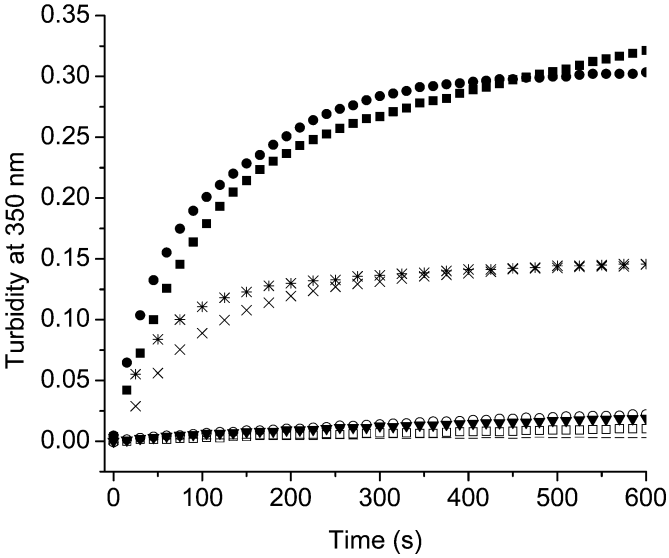

FIGURE 3: Effect of TMAO on microtubule assembly activity of tau[187] and [Y[310]A]tau[187]. Microtubules were assembled from purified tubulin (see Experimental Procedures) in the presence or absence of TMAO, wild-type tau[187], [Y[310]A]tau[187], or paclitaxel. Microtubule assembly was monitored by turbidity at OD_{350}. The initial conditions corresponding to each trace are 5 μM tubulin with the following: buffer alone (- - -), 0.2 M TMAO (▼), 1.5 μM tau[187] (○), 1.5 μM tau[187] and 0.2 M TMAO (●), 1.5 μM [Y[310]A]tau[187] (□), 1.5 μM [Y[310]A]tau[187] and 0.2 M TMAO (■), 5 μM paclitaxel (×), and 5 μM paclitaxel and 0.2 M TMAO (∗). The experiment was repeated more than three times.

T fluorescence, whose emission intensity is enhanced upon binding of the dye to tau aggregates. This method has been extensively used in previous studies of tau fiber formation (*23*, *45*) and is considered a specific test of amyloid formation in general (*46*). Using this assay, we found that tau[187] underwent heparin-induced aggregation with an initial rate (v_i) of 1753 cps/min (Figure 4A). In the presence of 0.2 or 1 M TMAO, the initial rate of aggregation was significantly enhanced (v_i = 15 685 or 99 541 cps/min, respectively) (Figure 4A). In the latter case, the initial rate of aggregation was enhanced 50-fold. To be sure that the aggregation process resulted in fiber formation, we visualized the final aggregates by electron microscopy. Negative stain electron microscopy (Figure 5A) showed that all filaments (after aggregation for 15 h) resembled straight filaments typical of those found in vivo, with diameters ranging from 17 to 28 nm and showing hints of twisting. Thus, TMAO accelerates the formation of filaments that appear similar in morphology to those classically observed in AD (*7*, *47*) (Figure 5B).

We determined the effect of TMAO on the critical concentration for aggregation of tau[187] by thioflavin T fluorescence or, alternatively, by solution turbidity measured by optical density at 350 nm. Results obtained by both methods were comparable. Heparin-induced aggregation to steady-state polymer mass was associated with a critical concentration of 3.8 μM tau in the absence of TMAO (Figure 6A). The critical concentration for tau was decreased to 1 μM in 0.2 M TMAO and to <1 μM in 1 M TMAO (Table 1). Thus, while TMAO appears to act principally by increasing the rate of aggregation, there was a significant effect on lowering the free energy of binding of tau[187] to the polymer end.

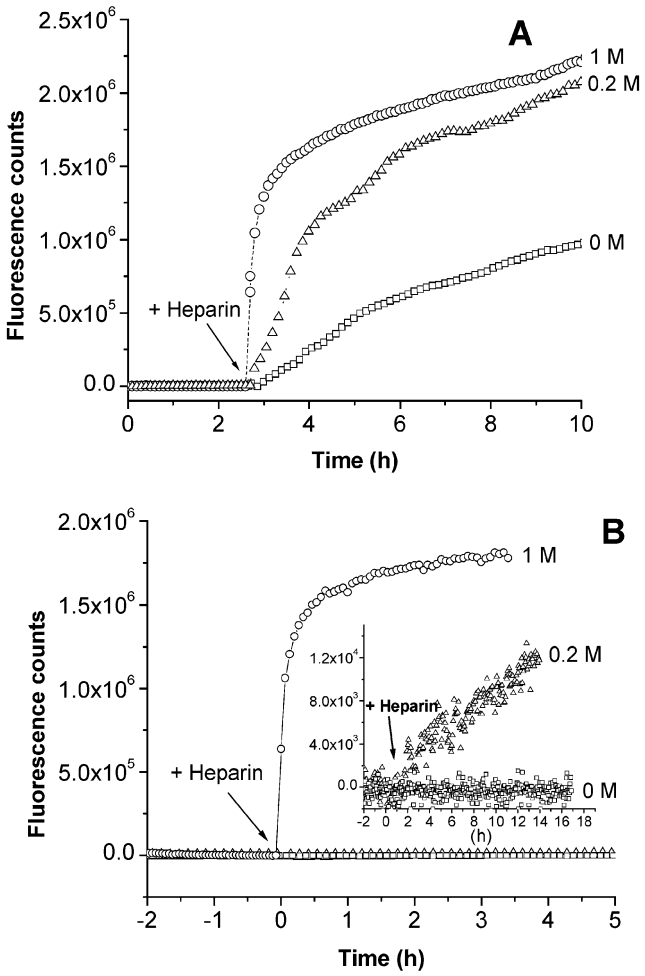

FIGURE 4: Effect of TMAO on heparin-induced aggregation of tau[187]. (A) Wild-type tau[187] or (B) [Y[310]A]tau[187] (each at 10 μM) was preincubated for approximately 2 h in aggregation buffer (see Experimental Procedures) containing 0 (□), 0.2 (△), or 1 M TMAO (○). Aggregation was then initiated by addition of heparin (0.11 mg/mL) (arrow), and aggregation was monitored by enhanced thioflavin T fluorescence. The inset in panel B shows a small but measurable increase in the aggregation rate of [Y[310]A]tau[187] in the presence of 0.2 M TMAO. The experiment was repeated more than three times.

Table 1: Effect of TMAO on the Critical Concentration for Aggregation of Wild-Type Tau[187] and [Y[310]A]Tau[187] [a]

experimental condition	critical concentration for wild-type tau[187] (μM)	critical concentration for [Y[310]A]tau[187] (μ M)
buffer	>100 [b]	>100 [b]
buffer and 2 M TMAO	>100 [b,c]	>100 [b,c]
buffer and heparin	3.8 ± 0.2	55.5 ± 0.5
buffer, heparin, and 0.2 M TMAO	1 ± 0.5	4.1 ± 1.1
buffer, heparin, and 1 M TMAO	<1	1.9 ± 0.2

[a] Wild-type tau[187] or [Y[310]A]tau[187] was incubated for 48 h at 25 °C in 20 mM potassium phosphate (pH 7.0) and 1 mM DTT under the specified conditions (0.11 mg/mL heparin). Aggregation was monitored by thioflavin T fluorescence by using an excitation wavelength of 450 nm and an emission wavelength of 480 nm. Mean values ± the standard deviation calculated from three independent experiments are reported. [b] No aggregation was detected; the reported value represents a lower limit on the critical concentration. [c] The same results were obtained at 0.2, 0.4, and 1 M TMAO.

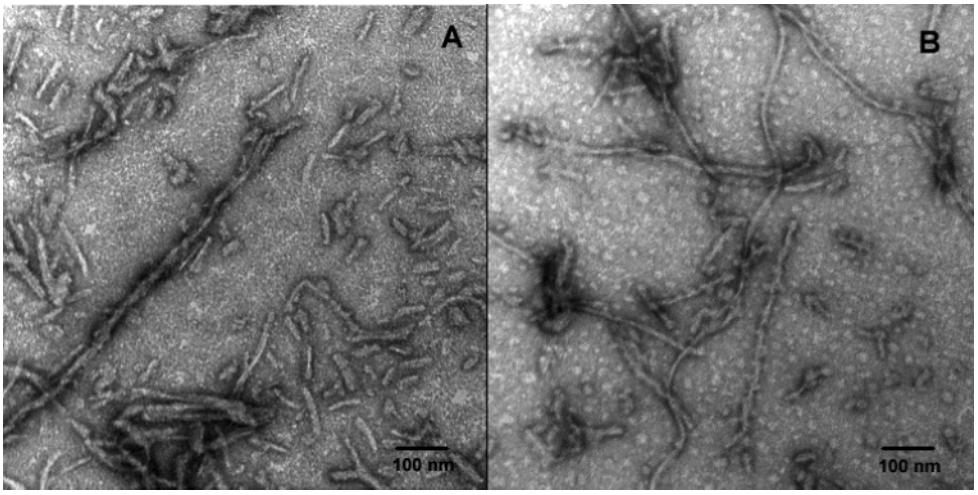

FIGURE 5: Transmission electron microscopy of fibers formed from tau^{187} in the absence or presence of TMAO. Wild-type tau^{187} was subjected to aggregation as described in the legend of Figure 1. (A) Fibers after aggregation for 20 h in buffer. (B) Fibers after aggregation for 20 h in buffer containing 0.2 M TMAO. The experiment was repeated more than three times.

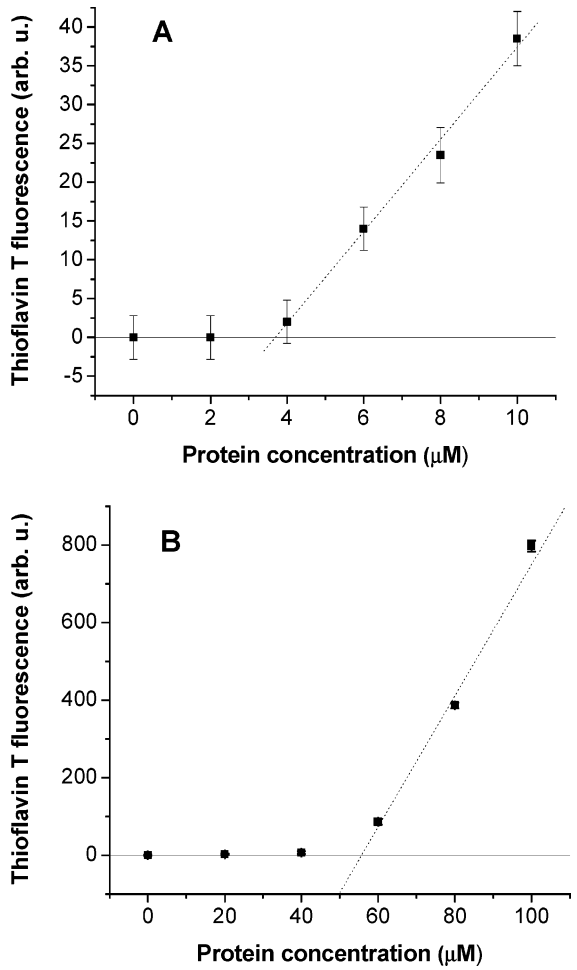

FIGURE 6: Determination of critical concentrations for (A) wild-type tau^{187} and (B) [Y^{310}A]tau^{187}. Proteins were incubated in 20 mM potassium phosphate buffer (pH 7.0), 1 mM DTT, and 0.11 mg/mL heparin for 48 h at 25 °C at the indicated concentrations. The relative amount of aggregated tau was determined by thioflavin T fluorescence by using an excitation wavelength of 450 nm and an emission wavelength of 480 nm. The dotted line represents the best fit to the experimental data. The error bars represent the standard deviation values calculated from three independent measurements. The critical concentration value is determined by extrapolation to the *x*-axis.

Role of Tyr^{310}. A region of six amino acids, ^{306}VQIVYK^{311}, within the microtubule-binding region of tau has previously been shown to be essential for the aggregation of tau in vitro (*3*). A single residue within this motif, Tyr^{310}, is critical (*45*). A critical role for tyrosyl residues in protein aggregation has been reported for the amyloid forming protein, acyl phosphatase, in which the most dramatic effects upon aggregation occurred upon individual substitution of two specific tyrosine residues in this protein (*48*). We therefore tested the role of Tyr^{310} in the aggregation of tau. When Tyr^{310} was changed to alanine, we found that in the absence of TMAO the resulting mutant ([Y^{310}A]tau^{187}) did not undergo heparin-induced aggregation (Figure 4B). However, in 0.2 M TMAO, the aggregation rate of the mutant (v_i = 31.8 cps/min) was slightly but measurably enhanced, while in 1 M TMAO, the initial rate of aggregation of the mutant (v_i = 106 384.73 cps/min) was completely restored to that of wild-type tau^{187} (Figure 4B). The source of the defect was a 14-fold elevated critical concentration in the mutant versus that of wild-type tau^{187}, and this defect was restored by TMAO (Table 1).

In contrast to its deleterious effects on aggregation, substitution of Tyr^{310} with alanine had virtually no effect on the ability of tau to promote MT assembly, either in the absence or in the presence of TMAO (Figure 3). This was true over a range of concentrations of the wild type and [Y^{310}A]tau^{187}. That is, at all concentrations that were tested, no significant differences between the wild type and mutant tau in terms of their ability to promote MT assembly were observed.

DISCUSSION

AD is characterized by the aggregation of tau, leading to appearance of the neurofibrillary tangles. While not proven, it is strongly believed that tau aggregation is critical to neurodegeneration. The biochemical mechanism that promotes tau folding in the aggregation process is not known; thus, agents or mutations that promote or hinder the aggregation pathway may serve as useful tools in investigating the aggregation mechanism. One such agent is the natural osmolyte, TMAO, which is noted for its ability to fold proteins into their native structures from an unstructured state, often with recovery of full biological activity (*26*, *31*). In

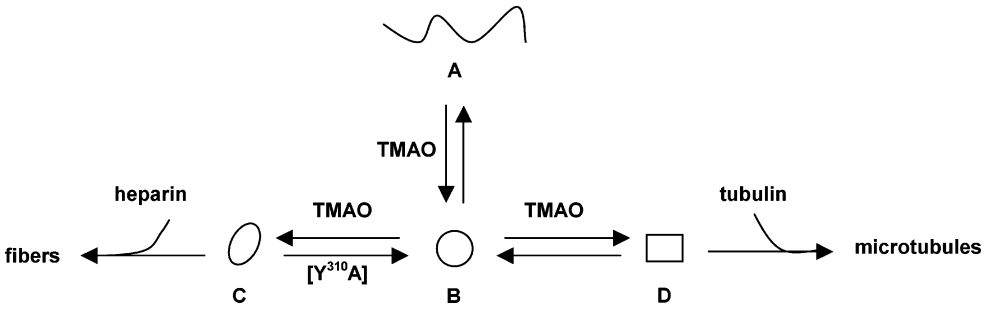

FIGURE 7: TMAO promotes both tau aggregation and tau-dependent MT assembly. Under native conditions, in the absence of TMAO, tau exists mainly as an unstructured polypeptide (A). We propose that addition of TMAO favors the formation of partially ordered intermediates (B, C, and D) that lie on the pathways to both aggregation and/or MT assembly. A point mutation, $Y^{310}A$, directly opposes the effects of TMAO on the aggregation, but not MT assembly, pathway. We propose that [C] ≪ [B]; hence, the mutation has no detectable effect on MT assembly.

this paper, we have shown that TMAO induces a structural reorganization in tau and accelerates both tau-dependent MT assembly and tau aggregation when tubulin and heparin, respectively, are present. Our long-term goal is to identify the structural elements induced by TMAO that are crucial for function.

It has been reported that TMAO does not accelerate the heparin-induced aggregation of human tau, using a tau construct that lacks the second N-terminal repeat sequence (*43*). In our hands, we found that TMAO at 1 M did enhance the aggregation of full-length human tau but that this rate enhancement was much attenuated compared to that of tau^{187} (not shown). In addition, a high concentration of TMAO caused little structural change in full-length tau as measured by CD spectroscopy, whereas tau^{187} displayed a significant gain in the level of secondary structure under these conditions. These observations are consistent with the N-terminal half of tau being inhibitory upon aggregation (R. George, unpublished data; *14*). One explanation may be that the N-terminus inhibits the structural changes necessary for aggregation by directly interacting with relevant structural determinants. We therefore chose tau^{187}, which lacks the N-terminus, as opposed to full-length tau as a model system in which to study changes in tau structure that are possibly linked to aggregation. Tau^{187} comprises all four MT-binding/repeat domains, assembles MTs, and undergoes aggregation to form fibers that are similar to those isolated from AD brain (Figure 5). TMAO not only dramatically enhances the initial aggregation rate of this fragment but also significantly lowers the critical concentration for polymerization. In a reversible polymerization process, the critical concentration is the concentration of free monomer during steady-state assembly/disassembly of the polymer and corresponds to the equilibrium dissociation constant (K_d) for the binding of free monomer to the polymer end (*49*). Thus, TMAO appears to enhance both the rate and affinity of binding of tau to the nucleus or fiber end to ultimately drive aggregation and/or fiber formation. This may be attributable to a net increase in the level of one or more intermediate species (B and C; see Figure 7) on the aggregation pathway induced by TMAO. The $Y^{310}A$ point mutation inhibits aggregation by increasing the critical concentration for aggregation, and this defect is reversed by TMAO. Notably, the same mutation has no effect on MT assembly, although TMAO enhances this process dramatically (*37*, *43*, *44*). We thus propose that while species C and B are on the aggregation pathway, B and D lie on the MT assembly pathway, and net interconversion of B and D is unchanged in the $Y^{310}A$ mutant (Figure 7).

TMAO has been shown to accelerate aggregation and fiber formation in both α-synuclein (*50*) and amyloid-β peptide (*51*). In our studies, we found that TMAO promotes the formation of critical structure(s) in tau which we believe are relevant to filament formation in vivo, because (1) aggregates of tau react with thioflavin T, suggesting that the induced structures are amyloid-like, and (2) filaments formed after aggregation for several hours display morphology similar to that of filaments isolated from AD brain tissue examined by EM. We speculate that in the absence of TMAO the structural conformers critical for aggregation or MT assembly are poorly populated and that TMAO induces their formation and the absence of heparin also traps them in soluble form (see Figure 7). This is based on our observation that in 2 M TMAO alone fiber formation is not induced (Table 1); rather, tau^{187} remains soluble, as demonstrated by high-speed centrifugation (not shown). The robust aggregation triggered by the subsequent addition of heparin suggests that TMAO serves to lower the free energy barrier of a rate-limiting step on the pathway to filament formation.

Substitution of a single amino acid, Tyr^{310}, with Ala profoundly compromises the ability of tau to aggregate yet has no effect on the structural changes induced by TMAO measured by CD (Figure 1). Thus, at least by this criterion, it is not envisioned that this substitution is likely to have a gross effect on protein folding. Tyr^{310} lies within the $VQIVY^{310}K$ motif which, as a sequence, has been shown to be essential for aggregation (*3*, *45*). This is likely due to the strong β-sheet inducing properties of V, Y, and I (*52*), as β-sheet propensity has been shown to strongly correlate with protein aggregation in general (*53*). The dramatically attenuated ability of $[Y^{310}A]tau^{187}$ to undergo aggregation is likely explained by the intrinsically weak preference for alanine in β-sheet structure (*52*). Another tau mutant, $Y^{310}E$, has also been shown to be defective in aggregation (*3*), consistent with the low β-sheet inducing propensity of Glu (*52*). However, compared to Ala and Glu, Phe is more similar to Tyr in β-sheet inducing propensity (*52*), and we found the $Y^{310}F$ -substituted mutant to be similar to the wild type in terms of aggregation rate (not shown).

The change in CD spectra of the mutant versus wild-type tau does not directly correlate with the respective changes in aggregation rate in response to TMAO. Therefore, we conclude that the specific conformer that is critical for

aggregation must not be observable by CD. Thus, while TMAO induces a significant gain in the level of secondary structure that can be observed by CD, the exact relationship between this gain in structure and the potential for aggregation is not known.

In summary, we propose that TMAO may induce some partial order in tau corresponding to multiple tau conformers that support either MT assembly in the presence of tubulin or alternatively aggregation in the presence of heparin (Figure 7). The ability of TMAO to rescue mutants that are defective in aggregation mirrors its ability to rescue disease-related mutations (*43*) or certain phosphorylated forms of tau (*37*, *42*), both of which confer defects in MT assembly. In the future, the use of TMAO in combination with high-resolution structural methods may provide an unprecedented glimpse into the structural basis for tau aggregation.

ACKNOWLEDGMENT

We are grateful for CD instrumentation kindly provided by Dr. Kevin Plaxco. We thank Dr. Rick Dalhquist for critical and invaluable discussions. We also thank Ana Misic for construction of the $Y^{310}A$ tau mutant and Hao Wang for technical assistance.

REFERENCES

1. Lee, V. M., Goedert, M., and Trojanowski, J. Q. (2001) Neurodegenerative tauopathies, *Annu. Rev. Neurosci. 24*, 1121−1159.
2. Avila, J., Lucas, J. J., Perez, M., and Hernandez, F. (2004) Role of tau protein in both physiological and pathological conditions, *Physiol. Rev. 84*, 361−384.
3. von Bergen, M., Friedhoff, P., Biernat, J., Heberle, J., Mandelkow, E. M., and Mandelkow, E. (2000) Assembly of tau protein into Alzheimer paired helical filaments depends on a local sequence motif (^{306}VQIVYK^{311}) forming β structure, *Proc. Natl. Acad. Sci. U.S.A. 97*, 5129−5134.
4. Schweers, O., Schonbrunn-Hanebeck, E., Marx, A., and Mandelkow, E. (1994) Structural studies of tau protein and Alzheimer paired helical filaments show no evidence for β-structure, *J. Biol. Chem. 269*, 24290−24297.
5. Cleveland, D. W., Hwo, S. Y., and Kirschner, M. W. (1977) Physical and chemical properties of purified tau factor and the role of tau in microtubule assembly, *J. Mol. Biol. 116*, 227−247.
6. Woody, R. W., Clark, D. C., Roberts, G. C., Martin, S. R., and Bayley, P. M. (1983) Molecular flexibility in microtubule proteins: Proton nuclear magnetic resonance characterization, *Biochemistry 22*, 2186−2192.
7. Wille, H., Drewes, G., Biernat, J., Mandelkow, E. M., and Mandelkow, E. (1992) Alzheimer-like paired helical filaments and antiparallel dimers formed from microtubule-associated protein tau in vitro, *J. Cell Biol. 118*, 573−584.
8. von Bergen, M., Barghorn, S., Li, L., Marx, A., Biernat, J., Mandelkow, E. M., and Mandelkow, E. (2001) Mutations of tau protein in frontotemporal dementia promote aggregation of paired helical filaments by enhancing local β-structure, *J. Biol. Chem. 276*, 48165−48174.
9. Berry, R. W., Abraha, A., Lagalwar, S., LaPointe, N., Gamblin, T. C., Cryns, V. L., and Binder, L. I. (2003) Inhibition of tau polymerization by its carboxy-terminal caspase cleavage fragment, *Biochemistry 42*, 8325−8331.
10. Minoura, K., Tomoo, K., Ishida, T., Hasegawa, H., Sasaki, M., and Taniguchi, T. (2002) Amphipathic helical behavior of the third repeat fragment in the tau microtubule-binding domain, studied by ^{1}H NMR spectroscopy, *Biochem. Biophys. Res. Commun. 294*, 210−214.
11. Esposito, G., Viglino, P., Novak, M., and Cattaneo, A. (2000) The solution structure of the C-terminal segment of tau protein, *J. Pept. Sci. 6*, 550−559.
12. Yanagawa, H., Chung, S. H., Ogawa, Y., Sato, K., Shibata-Seki, T., Masai, J., and Ishiguro, K. (1998) Protein anatomy: C-Tail region of human tau protein as a crucial structural element in Alzheimer's paired helical filament formation in vitro, *Biochemistry 37*, 1979−1988.
13. Mukrasch, M. D., Biernat, J., von Bergen, M., Griesinger, C., Mandelkow, E., and Zweckstetter, M. (2005) Sites of tau important for aggregation populate β-structure and bind to microtubules and polyanions, *J. Biol. Chem. 280*, 24978−24986.
14. Gamblin, T. C., Berry, R. W., and Binder, L. I. (2003) Modeling Tau Polymerization in Vitro: A Review and Synthesis, *Biochemistry 42*, 15009−15017.
15. Barghorn, S., Davies, P., and Mandelkow, E. (2004) Tau paired helical filaments from Alzheimer's disease brain and assembled in vitro are based on β-structure in the core domain, *Biochemistry 43*, 1694−1703.
16. Kirschner, D. A., Abraham, C., and Selkoe, D. J. (1986) X-ray diffraction from intraneuronal paired helical filaments and extraneuronal amyloid fibers in Alzheimer disease indicates cross-β conformation, *Proc. Natl. Acad. Sci. U.S.A. 83*, 503−507.
17. Giannetti, A. M., Lindwall, G., Chau, M. F., Radeke, M. J., Feinstein, S. C., and Kohlstaedt, L. A. (2000) Fibers of tau fragments, but not full length tau, exhibit a cross β-structure: Implications for the formation of paired helical filaments, *Protein Sci. 9*, 2427−2435.
18. Berriman, J., Serpell, L. C., Oberg, K. A., Fink, A. L., Goedert, M., and Crowther, R. A. (2003) Tau filaments from human brain and from in vitro assembly of recombinant protein show cross-β structure, *Proc. Natl. Acad. Sci. U.S.A. 100*, 9034−9038.
19. Margittai, M., and Langen, R. (2004) Template-assisted filament growth by parallel stacking of tau, *Proc. Natl. Acad. Sci. U.S.A. 101*, 10278−10283.
20. Goux, W. J. (2002) The conformations of filamentous and soluble tau associated with Alzheimer paired helical filaments, *Biochemistry 41*, 13798−13806.
21. Sadqi, M., Hernandez, F., Pan, U., Perez, M., Schaeberle, M. D., Avila, J., and Munoz, V. (2002) α-Helix structure in Alzheimer's disease aggregates of tau-protein, *Biochemistry 41*, 7150−7155.
22. Kuret, J., Chirita, C. N., Congdon, E. E., Kannanayakal, T., Li, G. B., Necula, M., Yin, H. S., and Zhong, Q. (2005) Pathways of tau fibrillization, *Biochim. Biophys. Acta 1739*, 167−178.
23. Chirita, C. N., and Kuret, J. (2004) Evidence for an intermediate in tau filament formation, *Biochemistry 43*, 1704−1714.
24. Anfinsen, C. B. (1973) Principles that govern the folding of protein chains, *Science 181*, 223−230.
25. Yancey, P. H., Clark, M. E., Hand, S. C., Bowlus, R. D., and Somero, G. N. (1982) Living with water stress: Evolution of osmolyte systems, *Science 217*, 1214−1222.
26. Bolen, D. W., and Baskakov, I. V. (2001) The osmophobic effect: Natural selection of a thermodynamic force in protein folding, *J. Mol. Biol. 310*, 955−963.
27. Wang, A., and Bolen, D. W. (1996) Effect of proline on lactate dehydrogenase activity: Testing the generality and scope of the compatibility paradigm, *Biophys. J. 71*, 2117−2122.
28. Hochachka, P. W., and Somero, G. N. (1968) The adaptation of enzymes to temperature, *Comp. Biochem. Physiol. 27*, 659−668.
29. Yancey, P. H., Rhea, M. D., Kemp, K. M., and Bailey, D. M. (2004) Trimethylamine oxide, betaine and other osmolytes in deep-sea animals: Depth trends and effects on enzymes under hydrostatic pressure, *Cell. Mol. Biol. (Paris, Fr., Print) 50*, 371−376.
30. Bell, J. D., Lee, J. A., Lee, H. A., Sadler, P. J., Wilkie, D. R., and Woodham, R. H. (1991) Nuclear magnetic resonance studies of blood plasma and urine from subjects with chronic renal failure: Identification of trimethylamine-*N*-oxide, *Biochim. Biophys. Acta 1096*, 101−107.
31. Kumar, R., Lee, J. C., Bolen, D. W., and Thompson, E. B. (2001) The conformation of the glucocorticoid receptor af1/tau1 domain induced by osmolyte binds co-regulatory proteins, *J. Biol. Chem. 276*, 18146−18152.
32. Tatzelt, J., Prusiner, S. B., and Welch, W. J. (1996) Chemical chaperones interfere with the formation of scrapie prion protein, *EMBO J. 15*, 6363−6373.
33. Tamarappoo, B. K., and Verkman, A. S. (1998) Defective aquaporin-2 trafficking in nephrogenic diabetes insipidus and correction by chemical chaperones, *J. Clin. Invest. 101*, 2257−2267.
34. Brown, C. R., Hong-Brown, L. Q., Biwersi, J., Verkman, A. S., and Welch, W. J. (1996) Chemical chaperones correct the mutant phenotype of the delta F508 cystic fibrosis transmembrane conductance regulator protein, *Cell Stress Chaperones 1*, 117−125.

35. Baskakov, I., and Bolen, D. W. (1998) Forcing thermodynamically unfolded proteins to fold, *J. Biol. Chem. 273*, 4831−4834.
36. Goode, B. L., Denis, P. E., Panda, D., Radeke, M. J., Miller, H. P., Wilson, L., and Feinstein, S. C. (1997) Functional interactions between the proline-rich and repeat regions of tau enhance microtubule binding and assembly, *Mol. Biol. Cell 8*, 353−365.
37. Tseng, H. C., Lu, Q., Henderson, E., and Graves, D. J. (1999) Phosphorylated tau can promote tubulin assembly, *Proc. Natl. Acad. Sci. U.S.A. 96*, 9503−9508.
38. Fulton, D. B., and Ni, F. (1997) ROESY with water flip back for high-field NMR of biomolecules, *J. Magn. Reson. 129*, 93−97.
39. Dalvit, C. (1998) Efficient multiple-solvent suppression for the study of the interactions of organic solvents with biomolecules, *J. Biomol. NMR 11*, 437−444.
40. Greenfield, N., and Fasman, G. D. (1969) Computed circular dichroism spectra for the evaluation of protein conformation, *Biochemistry 8*, 4108−4116.
41. Lendel, C., Dincbas-Renqvist, V., Flores, A., Wahlberg, E., Dogan, J., Nygren, P. A., and Hard, T. (2004) Biophysical characterization of Z(SPA-1): A phage-display selected binder to protein A, *Protein Sci. 13*, 2078−2088.
42. Tseng, H.-C., and Graves, D. J. (1998) Natural methylamine osmolytes, trimethylamine *N*-oxide and betaine, increase tau-induced polymerization of microtubules, *Biochem. Biophys. Res. Commun. 250*, 726−730.
43. Smith, M. J., Crowther, R. A., and Goedert, M. (2000) The natural osmolyte trimethylamine *N*-oxide (TMAO) restores the ability of mutant tau to promote microtubule assembly, *FEBS Lett. 484*, 265−270.
44. Eidenmuller, J., Fath, T., Hellwig, A., Reed, J., Sontag, E., and Brandt, R. (2000) Structural and functional implications of tau hyperphosphorylation: Information from phosphorylation-mimicking mutated tau proteins, *Biochemistry 39*, 13166−13175.
45. Goux, W. J., Kopplin, L., Nguyen, A. D., Leak, K., Rutkofsky, M., Shanmuganandam, V. D., Sharma, D., Inouye, H., and Kirschner, D. A. (2004) The formation of straight and twisted filaments from short tau peptides, *J. Biol. Chem. 279*, 26868−26875.
46. LeVine, H., III (1999) Quantification of β-sheet amyloid fibril structures with thioflavin T, *Methods Enzymol. 309*, 274−284.
47. Wisniewski, H. M., Merz, P. A., and Iqbal, K. (1984) Ultrastructure of paired helical filaments of Alzheimer's neurofibrillary tangle, *J. Neuropathol. Exp. Neurol. 43*, 643−656.
48. Chiti, F., Taddei, N., Baroni, F., Capanni, C., Stefani, M., Ramponi, G., and Dobson, C. M. (2002) Kinetic partitioning of protein folding and aggregation, *Nat. Struct. Biol. 9*, 137−143.
49. Kyte, J. (1995) *Structure in Protein Chemistry*, Garland Publishing, Inc., New York.
50. Uversky, V. N., Li, J., and Fink, A. L. (2001) Trimethylamine-*N*-oxide-induced folding of α-synuclein, *FEBS Lett. 509*, 31−35.
51. Yang, D. S., Yip, C. M., Huang, T. H., Chakrabartty, A., and Fraser, P. E. (1999) Manipulating the amyloid-β aggregation pathway with chemical chaperones, *J. Biol. Chem. 274*, 32970−32974.
52. Street, A. G., and Mayo, S. L. (1999) Intrinsic β-sheet propensities result from van der Waals interactions between side chains and the local backbone, *Proc. Natl. Acad. Sci. U.S.A. 96*, 9074−9076.
53. Chiti, F., Stefani, M., Taddei, N., Ramponi, G., and Dobson, C. M. (2003) Rationalization of the effects of mutations on peptide and protein aggregation rates, *Nature 424*, 805−808.

BI052167G